Volume 6 | Number 13 | 7 April 2015 | Pages 2359–2570

Polymer Chemistry

www.rsc.org/polymers

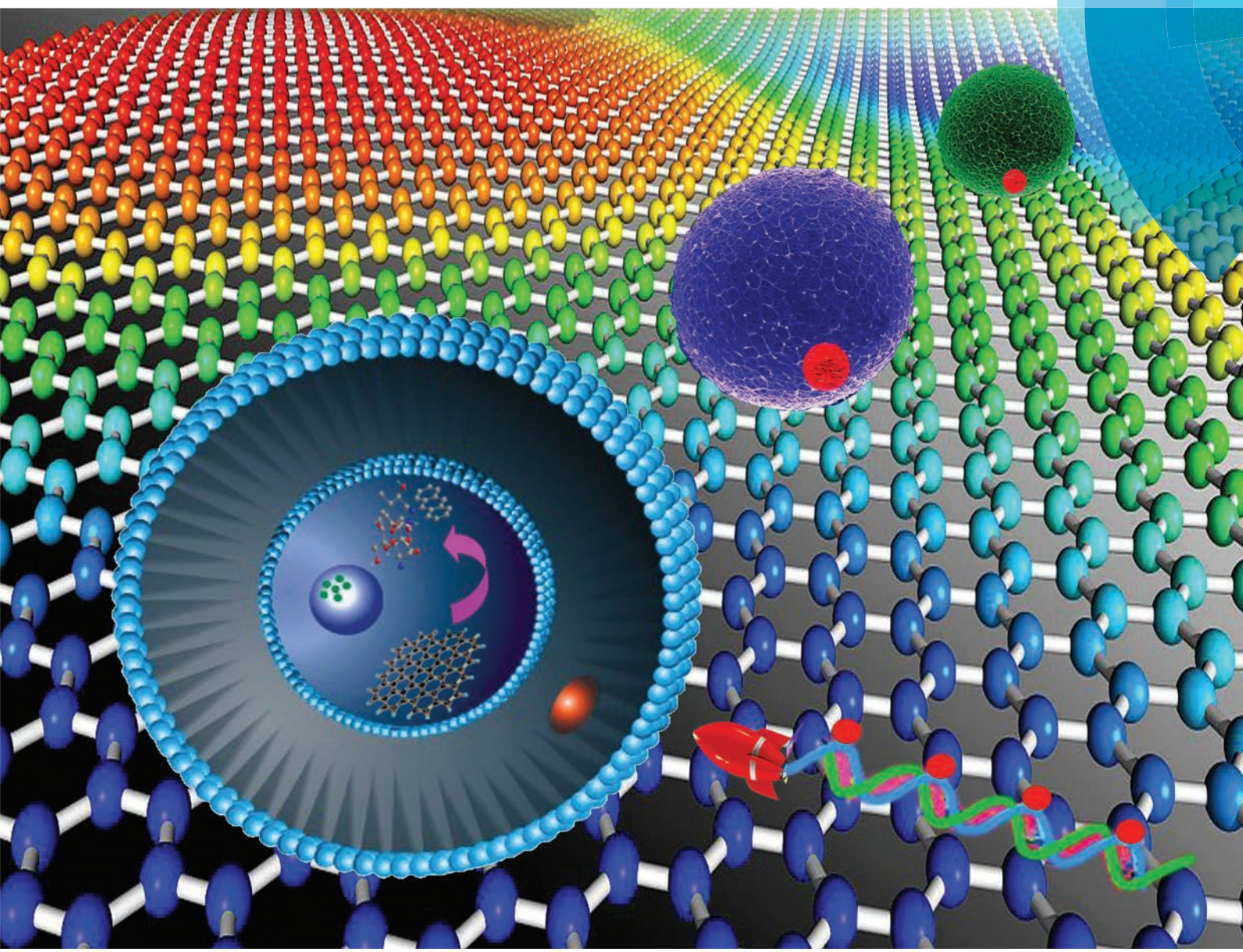

ISSN 1759-9954

ROYAL SOCIETY OF CHEMISTRY

PAPER
Yong Liu, Liming Dai *et al.*
Graphene oxide complex as a pH-sensitive antitumor drug

Polymer Chemistry

PAPER

View Article Online
View Journal | View Issue

Cite this: *Polym. Chem.*, 2015, **6**, 2401

Graphene oxide complex as a pH-sensitive antitumor drug†

Rumei Cheng,[a] Ruitao Zou,[a] Shengju Ou,[b] Rui Guo,[a] Ruiying Yan,[a] Haiyan Shi,[a] Shanshan Yu,[a] Xiaojian Li,[a] Yexu Bu,[a] Mimi Lin,[a] Yong Liu*[a] and Liming Dai*[a,c]

Received 14th January 2015,
Accepted 29th January 2015

DOI: 10.1039/c5py00047e

www.rsc.org/polymers

A pH-sensitive, nanostructured antitumor drug, GO-CONH-Schiff base (GCS), was prepared from the chitosan-xanthone Schiff base (CS)-modified graphene oxide (GO) complex. The successful synthesis of GCS was confirmed using various spectroscopic techniques, including FT-IR, XPS, UV-vis and TGA. The resulting GCS showed superb antitumor activity with the pH-sensitive release of the antitumor part, CS, and decreased cytotoxicity of GCS to normal human cells. The release of CS was stable and thorough in the solution at pH 1 (the pH value for gastric juice), suggesting that the as-synthesized, pH-sensitive drug could provide new insights into the design of advanced nanostructured oral drugs.

1. Introduction

Chitosan is an unbranched cationic biopolymer in acidic media because it carries a positive charge at pH below 6.5. Thus, chitosan shows attractive interactions with numerous negatively charged materials, such as most living tissues (*e.g.* skin, bone, hair), polysaccharides (*e.g.* alginate), polyanions, bacteria, fungi, enzymes and microbial cells. It has been shown that chitosan-based materials have many valuable bioactivities, including hemostasis, bacteriostasis, fungistasis, as well as anticancer and anticholesteremic activity.[1–3] Due to its well-known polymeric characters, chitosan has been used intensively in various drug delivery systems. For example, *N*-trimethyl chitosan chloride has been used as an effective gene carrier.[4,5] It has been found that this polymer can enhance the absorption of peptide and protein drugs across nasal[6] and intestinal epithelial cells.[7] Chitosan/folate-modified microcapsules with camptothecin have been reported for the targeted therapy of tumor cells.[8]

The application of chitosan as a drug for treatment of diseases, however, has not been realized because of its low pharmaceutical activity. Limited progress regarding the utilisation of modified chitosan as a potential drug has been reported. For instance, chitosan and its quaternized derivatives have been found to possess good antitumor, antimicrobial and antimycotic properties.[9] The formation of a Schiff base could enhance the pharmaceutical activities associated with chitosan.[10] Indeed, the citral-chitosan Schiff base was demonstrated to show higher antimicrobial activities than chitosan. Furthermore, the copper complex of the salicylaldehyde-chitosan Schiff base has been found to be strongly active against tumors.[11]

Herein, we synthesized a new class of chitosan-based antitumor drugs from a Schiff base formed by the coupling reaction between chitosan and xanthone. The combination of xanthone with chitosan improved the biological activity of the Schiff base, while the cationic property of chitosan enhanced the drug's permeability into tumor cells, providing additional advantages for the resulting antitumor drugs.

In this work, the unique 2D nanosheet graphene oxide (GO) was incorporated into the chitosan-xanthone Schiff base (CS) to further improve tumors' passive uptake of the polymer complexes *via* enhanced permeability and retention (EPR) effects.[12] Graphene-based materials have been widely studied for applications in biology, bioorganisms and biosensing.[13,14] Graphene-based nanomaterials have been reported to effectively inhibit the growth of *E. coli* while showing minimal cytotoxicity against normal cells.[15] Graphene-based networks or scaffolds have been found to provide a good biocompatible interface to support the growth and adhesion of live cells.[16,17] In particular, GO has been shown to be an effective carrier for delivering water-insoluble drugs into cells.[18,19]

It has been recognized that high biological effects of nanocomposites could be obtained from composites based on certain inorganic compounds and chitosan. For example, the

[a]*Institute of Advanced Materials for Nano-Bio Applications, School of Ophthalmology & Optometry, Wenzhou Medical University, 270 Xueyuan Xi Road, Wenzhou, Zhejiang 325027, China. E-mail: yongliu1980@hotmail.com*
[b]*Hangzhou Feipu Technology Co. Ltd, 525 Xixi Road, Hangzhou, Zhejiang 310023, China*
[c]*Center of Advanced Science and Engineering for Carbon (Case4Carbon), Department of Macromolecular Science and Engineering, Case Western Reserve University, 10900 Euclid Avenue, Cleveland, Ohio 44106, USA. E-mail: liming.dai@case.edu*

† Electronic supplementary information (ESI) available: AFM images of GCS and GO, High resolution XPS O 1s spectra of GO and GCS, TEM images of HeLa cells incubated with GCS. See DOI: 10.1039/c5py00047e

chitosan-PVP-TiO_2 nanocomposite can improve wound healing.[20] Gold nanoparticles are found to effectively facilitate the entry of chitosan-Pluronic into cells.[21] The most striking GO-chitosan nanocomposite stimulates the growth of osteoblasts whilst showing nontoxicity to normal cells.[22] Chitosan-modified GO composites as nanocarriers for anticancer drugs (*e.g.* camptothecin) and genes *via* π–π stacking and hydrophobic interactions have been realized, though the drug release is uncontrollable.[14] Of particular interest, chitosan-graphene dispersions have been found to be pH-responsive.[23] Therefore, the incorporation of GO with the chitosan Schiff base could provide additional pH sensitivity, which is useful for controlled release of the as-designed drugs. In this study, we have prepared a novel, nanostructured antitumor drug from the GO-CONH-Schiff base (GCS) compound, in which CS acted as the tumor inhibitor whilst GO worked as the drug delivery carrier. The resulting drug was further found to be pH-sensitive due to the presence of amines in its molecular structure. The release of CS from GCS was found to be pH-dependent, which would be useful for pH-triggered release at specific points and for the protection of drugs from degradation while passing through different organs and tissues. Our *in vitro* results suggest that the resulting GCS significantly inhibited the growth of HeLa cells. Successful fabrication of the resulting pH-sensitive antitumor drug provides new insights into the design of future nanostructured oral drugs.

2. Experimental

2.1 Materials

Graphite, with an average particle size of 100 μm, was obtained from Shanghai Reagent Co., Ltd GO used in our experiments was prepared according to Hummers' method.[24] Chitosan powders (with a deacetylation degree of 95% and viscosity of 200–400 mPa s), xanthenone (analytical grade), and acetic acid were all obtained from Aladdin Reagent Inc. Deionized water was collected from the Millipore purification system. All other chemicals were analytical grade and directly used without further purification.

2.2 Characterization

Fourier transform infrared (FT-IR) spectra were recorded on a PE Spectrum One spectrometer with KBr pellets in the 4000–450 cm^{-1} region. UV–vis spectra were measured on a PerkinElmer Lambda 35 spectrometer. Fluorescence emission spectra were obtained using an AB-series2 luminescence spectrometer. Atomic force microscopy (AFM) was carried out using a SPI3800N microscope operating in the tapping mode. Transmission electron microscopy (TEM) was characterised by a PHILIPS EM400ST microscope at an accelerating voltage of 150 kV. X-ray photoelectron spectra (XPS) were measured using ESCALAB MK-II spectrometer. Thermogravimetric analysis was performed by a STA 409 PC/4/H Lux at a heating rate of 10 °C per minute under N_2.

2.3 Synthesis of the chitosan-xanthone Schiff base (CS)

Chitosan powders (0.5 g) were dissolved in 100 mL aqueous solution of acetic acid (1 wt%) for 24 h and then transferred into a three-necked flask. 50 mL hot xanthone–ethanol solution was dropped into the flask, and 2 mL acetic acid was subsequently added. The mixture was refluxed at 70 °C for 18 h, followed by cooling down to room temperature. The product was neutralized with diluted NaOH, separated, and subsequently washed with deionized water and ethanol, respectively. The yield of the final product was found to be 80%.

2.4 Synthesis of the GO-CONH-Schiff base composite (GCS)

20 μL *N*-hydroxysuccinimide (NHS, 1.0 mM) and 20 μL of *N*-(3-dimethylaminopropyl)-*N*′-ethylcarbodiimide (EDC, 1.0 mM) solutions were added into the GO dispersion and remained for 10 min. 5 mM CS aqueous solution was subsequently introduced. The resulting solution was heated at 50 °C for 2 h and then stirred at room temperature for 12 h. Excess CS (precipitated as solid) was removed by centrifuge. The solution was then filtered using a Millipore filter (0.22 μm). GCS remaining in the filter was washed 4–6 times and redispersed in water. The schematic illustrations of CS and GCS are shown in Fig. 1.

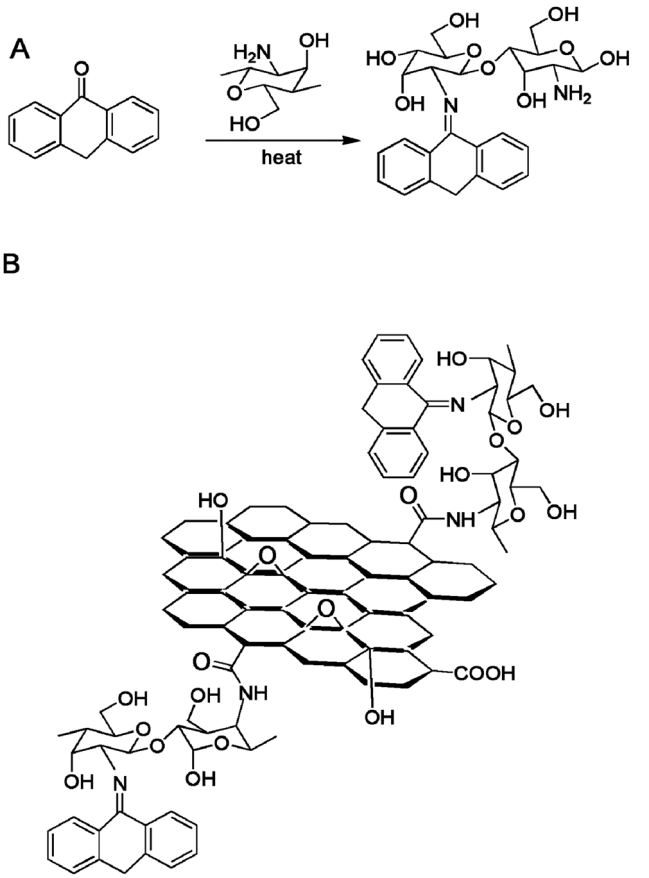

Fig. 1 (A) Schematic synthesis of CS and (B) schematic representation of the GCS nanocomposite.

2.5 The release of CS from GCS

To identify the xanthone contents in CS and GCS, two samples were subjected to 3 M HCl solutions. Xanthone was subsequently extracted by trichloromethane and determined by HPLC. To measure the release of CS from GCS, a calibration curve was first obtained using the fluorescence emission spectra at various pH levels. 50 mg GCS was then immersed in 10 mL solutions with different pH values. At predetermined time points, 1 mL of this solution was taken out and analysed for the released CS using luminescence spectrometry. 1 mL additional solution with the same pH was added to keep the total volume constant. The percentage of released CS was calculated from standard calibration curves.

2.6 Cell culture

HeLa cells were cultured in Dulbecco's modified Eagle's medium/F12 (12800-017, high glucose Gibco), supplemented with 10% fetal bovine serum (SV 30087.02, Hyclone) and 50 μg mL^{-1} gentamicin, in a humidified 5% CO_2 balanced air incubator at 37 °C. Medium was changed every 2 days. Cells were passaged with 0.25% trypsin (Invitrogen) plus 0.02% EDTA (Sigma). Cell viability was measured using the CCK8 assay. All samples were sterilized at a high temperature (120 °C). 4000 cells in 100 μL medium were seeded into each well of the 96-well culture plate. Sterilized samples were incubated with cells for 72 h. 10 μL CCK8 solution was then added into each well and incubated for 3 h. Absorbance was measured at the wavelength of 450 nm with a microplate reader (Biorad 680). The polystyrene (PS) surface of the 96-well culture plate was adopted as a negative control. Three repeats were done for each group.

3. Results and discussion

3.1 Characterization of CS and GCS

The successful incorporation of chitosan, xanthone and GO was confirmed using FT-IR spectroscopy. The differences in FT-IR spectra of chitosan before and after the synthesis are shown in Fig. 2(a) and (b). A broad peak at 3400 cm^{-1} from chitosan is associated with the coupled vibration of –OH and –NH_2. The peak at 3400 cm^{-1} became sharp in the spectrum of CS, which might be attributed to the breaking of hydrogen binding and subsequent formation of C=N. A new peak at 3280 cm^{-1} in the spectrum of CS arose from the unreacted –NH_2. The residual –NH_2 of CS further reacted with GO to form the GCS. Another –NH_2 peak presented at 1650 cm^{-1} both in chitosan and CS. Compared with the spectrum of chitosan, a new peak (1720 cm^{-1}) associated with the C=N double bond was observed for CS. Four peaks at 1556, 1350, 1268, and 953 cm^{-1} from the characteristic C=C vibration of aromatic rings were presented, confirming the successful synthesis of CS. Fig. 2(c) confirmed the formation of amide groups. It can be seen that the amide vibrations, appearing at 1657 and 1607 cm^{-1},[25] differed from the –NH_2 vibration at 1650 cm^{-1} as observed in both chitosan and CS. The peak at 3400 cm^{-1} turned broad again, suggesting the hydrogen binding of GO with chitosan. However, the vibration at 1720 cm^{-1} seen from CS was not well identified. It might be shielded by amide vibrations.

Formation of GCS nanocomposite was also confirmed by XPS analysis (Fig. 3). As shown in Fig. 3a, there were only C and O peaks presented in the XPS survey spectrum of GO, but C, N and O peaks were found in the XPS spectrum of GCS. Three peaks related to C–C (285.0 eV), C–O (286.4 eV), C=O (287.5 eV) and C(O)O (289.1 eV) groups were identified in the high-resolution C 1s spectrum of GO (Fig. 3b), while five bands associated with C–C (284.5 eV and 284.6 eV), C–N (285.8 eV), C–O (286.5 eV), C=N (287.9 eV) and N–C=O (288.7 eV) were fitted in the high-resolution C 1s spectrum of GCS (Fig. 3c). Two kinds of C–C bonds found for GCS were assigned to sp^3 carbons on the CS and GO, respectively. Another significant peak at 288.7 eV indicated the formation of amide from the covalent linkage of CS and GO. The C=O and C–O of GCS were identified at 531.2 eV and 532.9 eV, respectively, in the

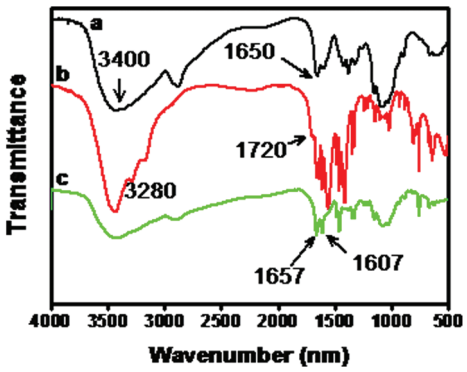

Fig. 2 FT-IR spectra of (a) chitosan, (b) CS, and (c) GCS.

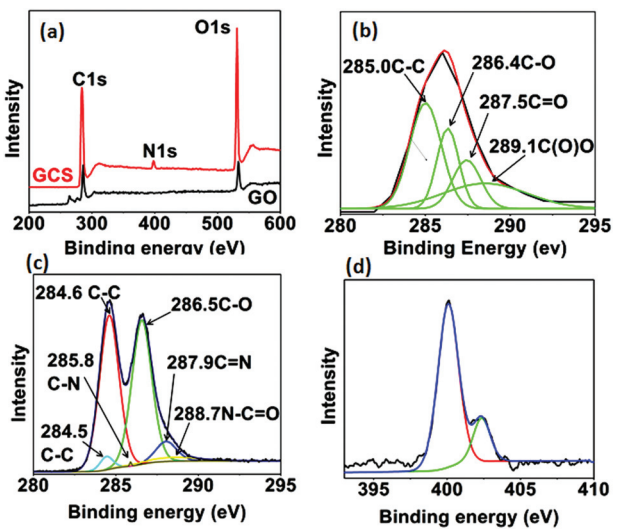

Fig. 3 (a) XPS survey spectra of GO and GCS; (b) high-resolution XPS C 1s spectrum of GO; (c) high-resolution XPS C 1s spectrum of GCS; (d) high-resolution XPS N 1s spectrum of GCS.

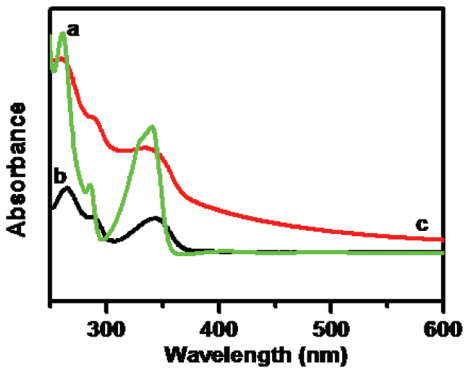

Fig. 4 UV-vis absorption spectra of (a) xanthone, (b) CS, and (c) GCS.

high-resolution O 1s spectrum (Fig. S2, ESI†). Typical C–N and C═N peaks at 400.1 and 402.2 were clearly observed in the high-resolution N 1s spectrum of GCS (Fig. 3d), suggesting presence of CS in the resulting GCS. XPS results further confirmed the successful synthesis of GCS.

UV-vis spectra of samples are shown in Fig. 4. Three characteristic peaks of xanthone were found at 261 nm, 285 nm, and 340 nm, associated with the π–π* electron transitions of aromatic rings.[26] When chitosan was introduced and the C═O at xanthone was replaced by the C═N, red shifts were observed. Three characteristic peaks of xanthone were found to shift to 265 nm, 288 nm, and 343 nm in the CS spectrum. After GO was incorporated with the CS, the GCS spectrum showed a very similar curve with that of the CS, but the absorption intensity significantly increased over a wide range of wavelength, presumably because the solubility of GCS has been remarkably increased by the newly grafted GO moieties.

Thermogravimetric analysis (TGA) was carried out to further confirm the successful synthesis of GCS. TGA is a very useful technique for the identification of various ingredients of a composite.[27,28] As shown in Fig. 5(a) and (b), the thermal stability of CS decreased when compared to chitosan. The weight loss of CS in the 50–130 °C range was attributed to the release of adsorbed water. The continuous weight loss above 180 °C was assigned to the breakdown of the –C═N bond and hydroxyl groups,[29] which was followed by glucose ring scissions and carbonization of the composite. After incorporation of GO into CS *via* amido bonds (Fig. 1), the TGA curve of GCS (Fig. 5c) showed a slower decomposition rate than that of CS, indicating greater thermo-stability of the resultant GCS. The physical mixture (MC) of CS and GO was also characterized to confirm covalent linkage between CS and GO in the as-prepared GCS. Difference between the resulting GCS and CS/GO MC was evident from the TGA results. The MC exhibited a lower weight loss rate and higher stability than GCS, since the MC did not have to break the amide groups. Compared to the TGA curves of CS and MC, the salient feature to be noticed on the TGA curve of GCS is the newly-appeared decomposition at *ca.* 470 °C, attributable to the weight loss caused by the scission of amide linkage between the GO and CS constituent components. These variations confirmed the successful chemical covalent linkage between CS and GO in the resulting GCS.

3.2 pH-dependent drug release

We further studied the fluorescence performance of CS, GCS and MC in aqueous solutions. Concentrations of xanthone groups in the three composites remained the same, since xanthone was the predominantly fluorescent group. A significant fluorescence quenching effect was observed for MC, presumably due to the FL quenching induced through the π–π stacking between the xanthone group in CS and GO (Fig. 6c).[30] Conversely, obvious florescence signals were obtained from both CS (Fig. 6a) and GCS (Fig. 6b). A higher fluorescence intensity was found for CS than that of GCS under identical conditions. This may be associated with formation of –CO–NH– bond in GCS, which significantly reduced FL quenching induced by the aforementioned π–π stacking, but still caused somewhat quenched fluorescence due to the photoinduced electron transfer (PET) effect.[31]

GCS further exhibited strong, pH-dependent fluorescence performance as shown in Fig. 7(a), comparable to that of the CS precursor (Fig. 7(b)). Higher fluorescence intensity obtained at the higher pH value could be attributed to the deprotonated amine atoms at the higher pH. In acidic solutions, protonation of the amine groups caused PET quenching of the fluorophore by the xanthone moiety, since the ener-

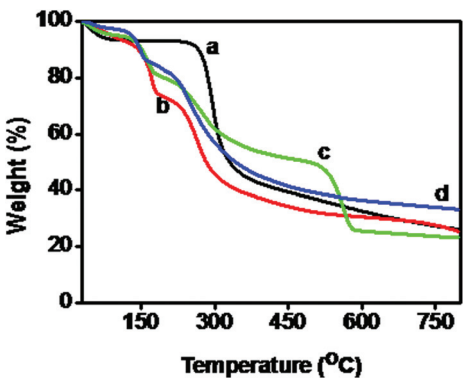

Fig. 5 TGA curves of (a) chitosan, (b) CS, and (c) GCS; (d) physical mixture of CS and GO.

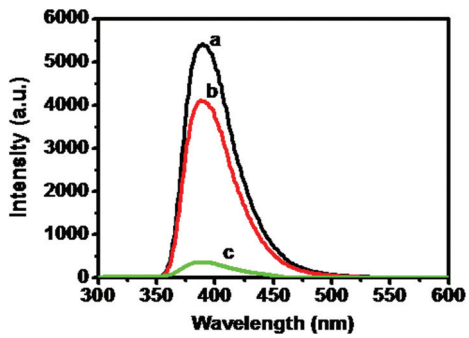

Fig. 6 Fluorescence spectra of (a) CS, (b) GCS, and (c) MC with the same concentrations of xanthone (pH = 6.0).

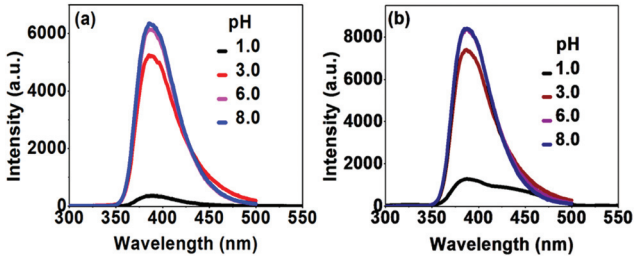

Fig. 7 pH-dependent fluorescence emission spectra of (a) GCS and (b) the pristine CS with the same concentration of xanthone.

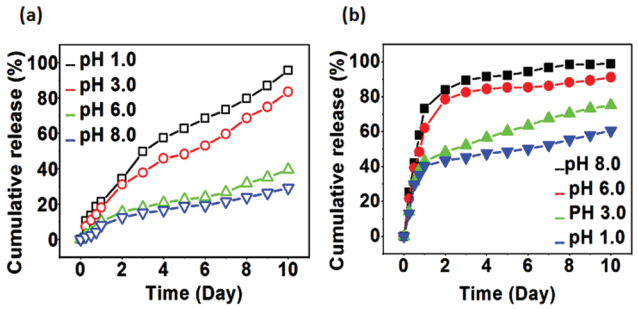

Fig. 8 (a) pH-dependent release of CS from the GCS; (b) pH-dependent release of CS from the MC physical mixture.

getics of the fluorophore was changed during the protonation process. This might have resulted in the quenched fluorescent intensity.[32]

The stability of the amido bond is diverse in solutions with different pH values. We thus investigated the pH-dependent release of CS from GCS. As shown in Fig. 8, the amounts of CS released increased with decreasing pH values. A total of 34.33%, 31.11%, 15.6%, and 12.4% CS was released from GCS by the second day in solutions with pH = 1, 3, 6 and 8, respectively. Released CS amounts gradually increased with increasing release time. This is because varied pH values influenced the breaking of amido bonds, resulting in the release of CS. For the purpose of comparison, the physical mixture MC was measured for controlled release at the identified conditions. It was found that the amounts of CS released increased with increasing pH values for MC, but release equilibrium was observed on the second day, suggesting poor sustained release capability and stability of the mixture without chemical covalent linkage. The CS release results suggest that the as-synthesized GCS exhibited superb pH-controlled and sustained release capability. Particularly, the lower pH value facilitated the release of GCS, suggesting great possibility for the resulting GCS to be a good candidate for oral administration, since the pH value of gastric juice is about 1.3.

3.3 Cytotoxicity with HeLa cells

Antitumor ability of the resulting GCS against HeLa cells were measured by CCK8 assay. For the purpose of comparison, xanthone and paclitaxel were also evaluated for cytotoxicity. Concentrations of CS and GCS were determined by the

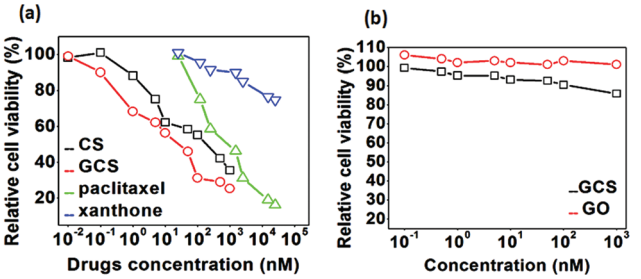

Fig. 9 (a) Relative cell viability (*versus* untreated control) of HeLa cells incubated with CS, GCS, paclitaxel and xanthone for 72 h; (b) relative cell viability data of human retina cells incubated with GCS and GO after incubation for 72 h.

amount of xanthone attached. It was found that xanthone and paclitaxel showed little toxicity with HeLa cells at relative high concentrations. As shown in Fig. 9(a), 2500 nM paclitaxel allowed 35% cell viability, while the same amount of xanthone resulted in more than 80% viability. Both CS and GCS, however, showed significantly antitumor effects even at the concentration of 10 nM, which induced nearly 50% HeLa cell apoptosis. When concentrations of both CS and GCS were increased to 1000 nM, only 35% and 25% live HeLa cells were observed, respectively. Particularly, stronger antitumor ability against HeLa cells was found for GCS compared to CS.

A better potential antitumor drug should possess high toxicity against tumor cells at low concentration, with low toxicity to normal human cells at high concentration. So we evaluated the biocompatibility of the as-prepared GCS with normal human retina cells. As shown in Fig. 9(b), over 85% human retina cells survived when the concentration of GCS was 1000 nM. Furthermore, no obvious toxicity against retina cells was obtained for different concentrations of GO without loading drugs, suggesting good biocompatibility of GO with normal retina cells. The results suggested that the incorporation of GO with CS enhanced the antitumor effect significantly, with low toxicity to normal cells, indicating that GO is suitable to be used as a nanocarrier. When the concentration of GCS was lower than 10 nM, the relative cell viability was over 93%, suggesting that the resulting GCS induced low toxicity to normal human cells.

4 Conclusions

In this work, we have synthesized a novel pH-sensitive antitumor drug from the chitosan-xanthone-graphene oxide (GCS) nanocomposite. Release of the CS antitumor parts from as-synthesized GCS showed superb pH-dependent properties, because changes in pH values resulted in the breakdown of amido bonds between GO and chitosan, leading to the controlled release of CS from GCS. CS was further found to be released stably and completely in the pH 1 solution, which is the pH value for gastric juice, suggesting the possibility of GCS to be orally administered. In addition, GCS exhibited excellent antitumor activity when compared with xanthone and pacli-

taxel. Our preliminary results present a simple but efficient way to prepare pH-controllable GCS antitumor drugs, which might open up great possibilities for the design of novel nanostructured oral drugs for various applications, such as detection and therapy of tumors.

Acknowledgements

Financial support for this work from the Chinese National Nature Science Foundation (21405115, 21374081, and 51433005), the National "Thousand Talents Program", Zhejiang Nature Science Foundation (LQ14C100002), Zhejiang Department of Education (Y201223055), and Wenzhou Bureau of Science and Technology (Y20120218) is acknowledged. L.D. is grateful for the support from NSF (CMMI-1266295).

Notes and references

1 M. N. V. Muzzarelli, R. A. A. Muzzarelli, C. Muzzarelli, H. Sashiwa and A. J. Domb, *Chem. Rev.*, 2004, **104**, 6017.
2 M. Dash, F. Chiellini, R. M. Ottenbrite and E. Chiellini, *Prog. Polym. Sci.*, 2011, **36**, 981.
3 L. Hu, Y. Sun and Y. Wu, *Nanoscale*, 2013, **5**, 3103.
4 A. B. Sieval, M. Thanou, A. F. Kotzé, J. E. Verhoef, J. Brussee and H. E. Junginger, *Carbohydr. Polym.*, 1998, **36**, 157.
5 M. Thanou, B. I. Florea, M. Geldof, H. E. Junginger and G. Borchard, *Biomaterials*, 2002, **23**, 153.
6 L. Illum, N. F. Farray and S. S. Davis, *Pharm. Res.*, 1994, **11**, 1186.
7 P. Artursson, T. Lindmark, S. S. Davis and L. Illum, *Pharm. Res.*, 1994, **11**, 1358.
8 A. Galbiati, C. Tabolacci, B. M. Della Rocca, P. Mattioli, S. Beninati, G. Paradossi and A. Desideri, *Bioconjugate Chem.*, 2011, **22**, 1066.
9 C. H. Kim, J. W. Choi, H. J. Chun and K. S. Choi, *Polym. Bull.*, 1997, **38**, 387.
10 X. Jin, J. Wang and J. Bai, *Carbohydr. Res.*, 2009, **344**, 825.
11 R. M. Wang, P. H. Nai, P. F. Song, Y. F. He, L. Ding and Z. Q. Lei, *Polym. Adv. Technol.*, 2008, **20**, 959.
12 K. Yang, S. Zhang, G. Zhang, X. Sun, S. T. Lee and Z. Liu, *Nano Lett.*, 2010, **10**, 3318.
13 Y. Wang, Z. Li, J. Wang, J. Li and Y. Lin, *Trends Biotechnol.*, 2011, **29**, 205.
14 H. Bao, Y. Pan, Y. Ping, N. G. Sahoo, T. Wu, L. Li, J. Li and L. H. Gan, *Small*, 2011, **7**, 1569.
15 W. B. Hu, C. Peng, W. J. Luo, M. Lv, X. M. Li, D. Li, Q. Huang and C. H. Fan, *ACS Nano*, 2010, **4**, 4317.
16 S. Agarwal, X. Zhou, F. Ye, Q. He, G. C. K. Chen, J. Soo, F. Boey, H. Zhang and P. Chen, *Langmuir*, 2010, **26**, 2244.
17 H. Chen, M. B. Müler, K. J. Gilmore, G. Wallace and D. Li, *Adv. Mater.*, 2008, **20**, 3557.
18 X. Sun, Z. Liu, K. Welsher, J. Robinson, A. Goodwin, S. Zaric and H. Dai, *Nano Res.*, 2008, **1**, 203.
19 Z. Liu, J. T. Robinson, X. Sun and H. Dai, *J. Am. Chem. Soc.*, 2008, **130**, 10876.
20 D. Archana, B. K. Singh, J. Dutta and P. K. Dutta, *Carbohydr. Polym.*, 2013, **95**, 530.
21 K. S. Oh, R. S. Kim, J. Lee, D. Kimg, S. H. Cho and S. H. Yuk, *J. Appl. Polym. Sci.*, 2008, **108**, 3239.
22 D. Depan, B. Girase, J. S. Shah and R. D. K. Misra, *Acta Biomater.*, 2011, **7**, 3432.
23 M. Fang, J. Long, W. Zhao, L. Wang and G. Chen, *Langmuir*, 2010, **26**, 16771.
24 W. S. Hummers Jr. and R. E. Offeman, *J. Am. Chem. Soc.*, 1958, **80**, 1339.
25 P. H. Chen, T. Y. Kuo, J. Y. Kuo, Y. P. Tseng, D. M. Wang, J. Y. Lai and H. J. Hsieh, *Carbohydr. Polym.*, 2010, **82**, 1236.
26 Y. S. Zou, A. J. Hou, G. F. Zhu, Y. F. Chen, H. D. Sun and Q. S. Zhao, *Bioorg. Med. Chem.*, 2004, **12**, 1947.
27 D. A. Kron, B. T. Hollan, R. Wipson, C. Mareke and A. Stein, *Langmuir*, 1999, **15**, 8300.
28 G. Moroi, *React. Funct. Polym.*, 2008, **68**, 268.
29 A. Patel and K. Mequanint, *Polymer*, 2009, **50**, 4464.
30 E. Bozkurt, M. Acar, Y. Onganer and K. Meral, *Phys. Chem. Chem. Phys.*, 2014, **16**, 18276.
31 A. P. De Silva, D. B. Fox, A. J. M. Huxley and T. S. Moody, *Coord. Chem. Rev.*, 2000, **205**, 41.
32 A. P. De Silva, H. Q. N. Gunaratne and C. P. McCoy, *J. Am. Chem. Soc.*, 1997, **119**, 7891.

